

Electron-scattering mechanisms in single-crystal K_3C_{60}

Vincent H. Crespi, J. G. Hou, X.-D. Xiang, Marvin L. Cohen, and A. Zettl

*Department of Physics, University of California at Berkeley, Berkeley, California 94720
and Materials Sciences Division, Lawrence Berkeley Laboratory, Berkeley, California 94720*

(Received 20 May 1992)

The temperature-dependent resistivity of single-crystal K_3C_{60} is studied from the point of view of electron-electron and electron-phonon scattering. The electron-phonon analysis suggests that conventional electron-phonon coupling would be sufficient to account for the superconductivity, with contributions to the coupling from both high-frequency intraball and low-frequency interball modes. The resistivity was also compared to a quadratic temperature dependence, suggestive of electron-electron scattering at anomalously high temperatures.

Determination of the transport mechanisms in alkali-doped C_{60} can provide valuable information pertinent to superconductivity. Recent transport measurements^{1,2} for single crystals of K_3C_{60} have been analyzed in terms of both electron-electron and electron-phonon scattering processes. For simplicity, it is assumed that one or the other mechanism is dominant, so as to elucidate the primary physical consequences of either scattering process.

The small bandwidth and large on-site Coulomb interaction³ in the doped fullerenes suggest a role for electron-electron interactions. The standard treatment of electron-electron scattering yields a T^2 temperature dependence from phase-space factors. Motivated by these considerations, the resistivity data have been fit to a form $\rho(T) = a + bT^2$, shown as the solid line in Fig. 1. A log-log plot of the raw experimental data actually yields a slope of 1.73. The situation is reminiscent of the organic conductors, several of which exhibit a nearly quadratic temperature dependence up to high temperatures.⁴ The theoretical T^2 dependence assumes constant volume. Thermal expansion should increase the density of states at the Fermi level, producing a resistivity $\rho(T) = a + b[N_0(T)T]^2$, where $N_0(T)$ is the temperature-dependent density of states at the Fermi level. We have taken account of this effect by combining thermal expansion data for *undoped* C_{60} (Ref. 5) and density of states versus lattice constant results from a pseudopotential calculation.⁶ The quality of the fit decreases, as evidenced by the dashed line in Fig. 1. The inset shows a log-log plot of the resistivity data corrected for thermal expansion compared to a line of slope 2. The thermally corrected data have a shallower slope and are slightly nonlinear. We note theoretical results that suggest that metallic screening could be very efficient.⁷ The possible relevance of electron-electron scattering could be further tested by examining the robustness of the near-quadratic temperature dependence at different lattice constants.

We next examine the data from the point of view of electron-phonon coupling. We begin with the Ziman resistivity formula,⁸

$$\rho(T) = \frac{8\pi^2}{\omega_p^2 k_B T} \int_0^{\omega_{\max}} \frac{\hbar\omega \alpha_{tr}^2 F(\omega)}{\cosh\left(\frac{\hbar\omega}{k_B T}\right) - 1} d\omega, \quad (1)$$

which relates the resistivity to the transport electron-phonon coupling function $\alpha_{tr}^2 F(\omega)$. In most cases $\alpha_{tr}^2 F(\omega)$ provides a reasonable approximation to $\alpha^2 F(\omega)$, the expression relevant to superconductivity. The transport expression weighs the differences in Fermi velocities between different points on the Fermi surface. The two expressions could be significantly different if the electron-phonon matrix elements have a strong dependence on wave vector. However, the intramolecular phonons should exhibit very little dispersion, strongly suggesting that the electron-phonon coupling for these modes is isotropic in k space. Orientational disorder⁹ should further encourage isotropic coupling. The situa-

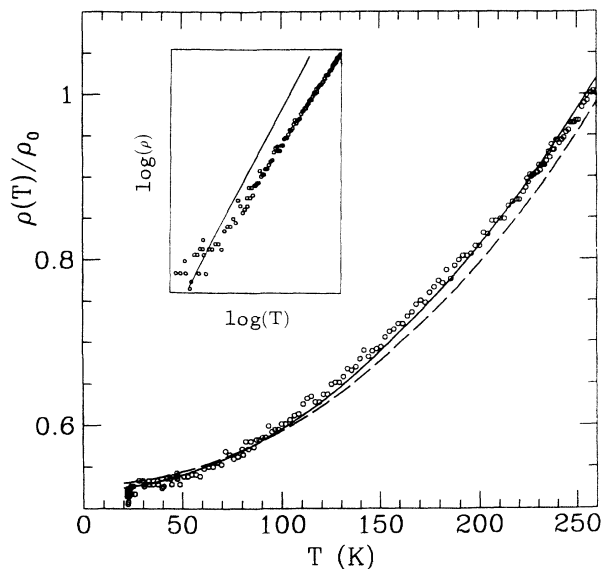


FIG. 1. Fits of theoretical electron-electron scattering models to the experimental resistivity (circles). The solid line is a fit to the form $a + bT^2$. The dashed line is a fit to the form $a + b[N_0(T)T]^2$, where $N_0(T)$ is the temperature-dependent density of states. The experimental data has been normalized to the value at $T = 260$ K. The inset shows a log-log plot of the resistivity after correction for thermal expansion compared to a line of slope 2.

tion is less clear for the lower-frequency librational, vibrational, and alkali modes. Phase-space factors suggest that phonons along Cartesian directions will be preferentially weighed in the electron-phonon coupling integral.¹⁰ These nesting phonons have two flavors: those that bridge across necks of the Fermi surface and those that nest along the flat sides of these necks. The first (second) variety yields fairly large (small) differences in Fermi velocities. If the electron-phonon matrix elements for the low-frequency phonons are anomalously large or small for either variety of nesting wave vector, then these modes could contribute to $\alpha_{tr}^2 F(\omega)$ and $\alpha^2 F(\omega)$ to differing degrees. As a caveat, the phase-space results assume orientational order, at variance with experiment.⁹

The Ziman formula assumes an isotropic, energy-independent scattering time. A fcc crystal such as K_3C_{60} should be reasonably isotropic. The approximation of an energy-independent scattering time typically overestimates the resistivity at intermediate temperatures.⁸ In addition, the Bloch-Boltzmann transport formalism assumes that $N(0)\omega_{\text{Debye}}$ is small,¹¹ a questionable assumption for a system with high phonon frequencies and a potentially large density of states. A final concern is that the Bloch-Boltzmann theory fails for mean free paths on the order of the interatomic spacing. Recent upper critical field measurements on single-crystal samples imply a $T = 0$ mean free path on the order of 27 \AA ,² substantially larger than the interatomic separation and somewhat larger than the intermolecular spacing.

Before analyzing the experimental resistivity data, we discuss the importance of the absolute magnitude of the resistivity to the calculations. Experimental geometrical uncertainties make an accurate determination of the resistivity problematical. For this reason, we appeal to an analysis of upper critical field data, which yields a scattering time of $1.7 \pm 0.5 \times 10^{-14}$ sec (Ref. 2). The scattering time measurement determines the overall scale of the electron-phonon coupling, while the functional form of the temperature-dependent resistivity provides a constraint on the frequency distribution of the electron-phonon coupling.

In order to gain a measure of physical insight into the form of $\alpha_{tr}^2 F(\omega)$, we first fit the data with a δ function form, $\alpha_{tr}^2 F(\omega) = \frac{1}{2} \lambda \omega \delta(\omega - \bar{\omega})$, yielding $\bar{\omega} \approx 400$ K and $\lambda \approx 0.6$. This drastic simplifying assumption is not directly physically relevant. However, the simple fit implies that a more physical analysis should involve modes with frequencies both above and below 400 K.

To proceed further, we consider various theoretical calculations for the electron-phonon coupling. The model of Jishi and Dresselhaus¹² (JD) emphasizes the lower-frequency radial intramolecular modes, producing an average frequency of roughly 500 K and $\lambda \approx 1$. The models of Schluter *et al.*¹³ (SLNB) involve contributions from a broad range of H_g modes with an average frequency of $\omega_{\text{log}} \sim 1000$ K and $\lambda \approx 0.6$. The particular model chosen for detailed analysis is the first listed in Table I of Ref. 13. In contrast, the calculations of Varma *et al.*¹⁴ (VZR) yield significant coupling only to the two highest H_g modes at frequencies near 2000 K, with $\lambda \approx 0.5$. These models are evaluated by two criteria: the corre-

spondence of the theoretical and experimental temperature dependences, and the magnitude of λ necessary to reproduce the experimentally measured resistivity. For each model, the overall coupling strength and the residual resistivity were adjusted in a least-squares fit to the data.

Referring to Fig. 2, JD produce a reasonable fit to the temperature dependence over the range 0–260 K. At high temperatures the theoretical curve has a somewhat smaller slope than the experimental results. SLNB and VZR do not adequately reproduce the measured temperature dependence. The quality of the fits is decreased further if the residual resistivity is fixed at the experimental value. The insufficient curvature at low temperatures suggests additional coupling at a lower frequency. Motivated by this consideration, we include a lower-frequency contribution of adjustable strength, with the results presented in Fig. 3. The new phonon mode was set at a frequency of 150 K, but the quality of the fit and the magnitude of the coupling to this lower mode are roughly unchanged for frequencies in the range 20–200 K. For SLNB and VZR, this modification greatly improves the agreement with experiment. This result is not an artifact of the additional free parameter; the fit is not improved if the additional mode is placed at a frequency above 400 K. Within the accuracy of the analysis, these three models yield agreement with experiment which is comparable to that obtained by the electron-electron analysis.

Is there a physical motivation for the inclusion of a lower-frequency mode? A simple calculation yields an estimate of λ for intermolecular translational modes. Within a tight-binding model, the bandwidth W varies as an overlap integral between electronic states $\phi(\mathbf{r})$ and $\phi(\mathbf{r} + \mathbf{R})$. Consider the change in the overlap integral under a change in lattice constant, where we assume that

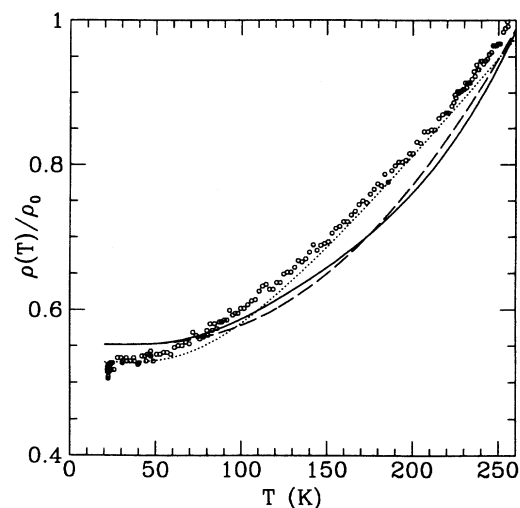


FIG. 2. Fits of theoretical electron-phonon scattering models to the experimental resistivity (circles). The solid, dashed, and dotted lines are for the models VZR (Ref. 14), SLNB (Ref. 13), and JD (Ref. 12), respectively. The data have been normalized to the value at $T = 260$ K.

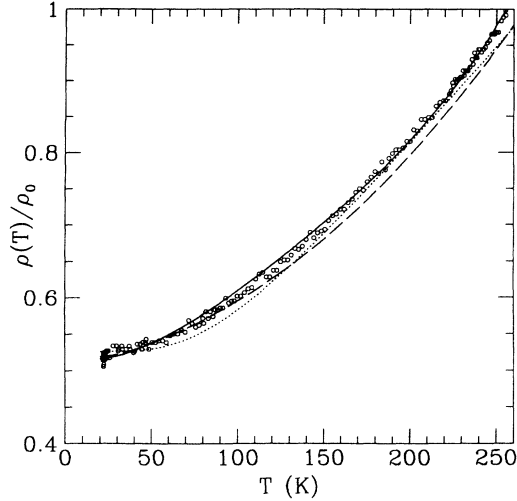


FIG. 3. Fits of theoretical electron-phonon models with an additional phonon mode at 150 K. The curve assignments are the same as Fig. 2.

the fullerene electronic states are unchanged,

$$\delta W \sim \int \phi^*(\mathbf{r}) \delta U(\mathbf{r}) \phi(\mathbf{r} + \mathbf{R}) d\mathbf{r}, \quad (2)$$

where $U(r)$ is the deviation from superposed molecular potentials. This expression has the same form as a real-space formulation for the McMillan-Hopfield parameter $\langle I^2 \rangle$, which enters the expression for λ as $\lambda = \frac{N(0)\langle I^2 \rangle}{M\langle \omega^2 \rangle}$,¹⁵ where $\langle \omega^2 \rangle$ is an average squared phonon frequency, M is the molecular mass, and $N(0)$ is the density of states at the Fermi level. A low- q longitudinal intermolecular vibrational phonon will produce a local change in the lattice constant. Using pseudopotential calculations to estimate the bandwidth and change in density of states upon lattice contraction,⁶ we approximate λ by the expression $\lambda \sim W^2 \left(\frac{\delta N}{\delta a} \right)^2 / NM \langle \omega^2 \rangle$, which yields λ of order 0.1 for a mode of frequency ~ 100 K. More sophisticated tight-binding calculations for high- q intermolecular modes indicate large changes in the band structure, indicative of significant electron-phonon coupling.¹⁶ Low-frequency librational modes could also exhibit significant coupling, since the overlap integrals between C_{60} molecules will be sensitive functions of their relative orientations.¹⁷ Polarization of the C_{60} molecules by alkali atom vibrations could also produce a low-frequency contribution to the electron-phonon coupling.¹⁸

The resistivity has also been fit to an $\alpha^2 F(\omega)$ corresponding to a uniformly scaled version of the inelastic neutron scattering intensity.¹⁹ The approximation of constant coupling strength is unlikely to be valid, since the scattering data includes modes of qualitatively distinct character. In fact, this naive fit yields too strong a temperature dependence at low temperatures, indicating excessive coupling to low-frequency modes. If the modes below 25 meV are removed by hand, the fit is too flat

at low temperatures, suggesting that the lower frequency modes contribute to the scattering process, but less so than implied by the magnitudes of the peaks in the neutron scattering.

Table I shows the values of λ deduced from the fits to the resistivity data for each of the theoretical forms for $\alpha^2 F(\omega)$. The range of values corresponds to a scattering time in the range $1.7 \pm 0.5 \times 10^{-14}$ sec. JD yield λ slightly lower than that required to produce the observed T_c , whereas VZR yields λ too big. These results suggest that an electron-phonon model for superconductivity should include contributions from a range of intramolecular vibrations.

A correction for the effect of thermal expansion on the density of states yields a 10–15% reduction in the coupling to the higher-frequency modes and little change in the coupling to the lower-frequency mode. These changes do not substantively alter the conclusions of the analysis. The temperature dependence of the resistivity is reproduced to the same accuracy with or without the treatment of thermal expansion.

An estimate based on theoretical results for other superconductors²⁰ suggests that the preceding analysis will yield a near-BCS gap ratio of $\frac{2\Delta}{k_B T_c} \approx 3.6 - 4.0$. Preliminary tunneling measurements yield $\frac{2\Delta}{k_B T_c} = 5.3$,²¹ while infrared measurements suggest $\frac{2\Delta}{k_B T_c} \sim 3 - 5$.²² It has been suggested that strong coupling to low-frequency vibrational modes could account for a large gap ratio.¹⁷ The unambiguous determination of this important superconducting parameter merits further effort.

In conclusion, an analysis of resistivity data on doped single crystals of K_3C_{60} suggests that the superconductivity is consistent with conventional electron-phonon coupling involving a range of intramolecular phonons. Within this analysis, the coupling strength to lower-frequency modes does not contribute significantly to either the superconducting transition temperature or the gap ratio.

Note added in proof. Recent measurements of the optical reflectivity of K_3C_{60} and Rb_3C_{60} imply a near-BCS gap ratio.²³

TABLE I. Best-fit values of λ to the temperature-dependent resistivity for various theoretical models of the electron-phonon coupling. The appellation “low” refers to a coupling function with an additional low-frequency mode at 150 K. The appellation “thermal” implies that a correction for thermal expansion has been applied.

Model	λ_{high}	λ_{low}
SLNB	0.9–1.7	
SLNB (low)	0.6–1.1	0.1–0.17
SLNB (low,thermal)	0.5–0.9	0.1–0.17
VZR	2.0–3.6	
VZR (low)	1.4–2.5	0.1–0.17
VZR (low,thermal)	1.2–2.1	0.1–0.2
JD	0.4–0.6	
JD (low)	0.4–0.6	0.01–0.02
JD (low,thermal)	0.3–0.5	0.03–0.04

ACKNOWLEDGMENTS

This research was supported by National Science Foundation Grant No. DMR-9120269 and by the Office of En-

ergy Research, Office of Basic Energy Sciences, Materials Sciences Division of the U. S. Department of Energy under Contract No. DE-AC03-76SF00098. V.H.C. was supported by the National Science Foundation and the Department of Defense.

-
- ¹X.-D. Xiang, J. G. Hou, G. Briceño, W. A. Vareka, R. Mostovoy, A. Zettl, V. H. Crespi, and M. L. Cohen, *Science* **256**, 1190 (1992).
- ²J. G. Hou, V. H. Crespi, X.-D. Xiang, W. A. Vareka, G. Briceño, A. Zettl, and M. L. Cohen (unpublished).
- ³V. de Coulon, J. L. Martins, and F. Reuse, *Phys. Rev. B* **45**, 13 671 (1992).
- ⁴T. Ishiguro and K. Yamaji, *Organic Superconductors* (Springer-Verlag, Berlin, 1990), p. 36.
- ⁵W. I. F. David, R. M. Ibberson, T. J. S. Dennis, J. P. Hare, and K. Prassides, *Europhys. Lett.* **18**, 219 (1992).
- ⁶A. Oshiyama and S. Saito, *Solid State Commun.* **82**, 41 (1992).
- ⁷O. Gunnarsson and G. Zwicknagl, *Phys. Rev. Lett.* **69**, 957 (1992).
- ⁸G. Grimvall, *The Electron-Phonon Interaction in Metals* (North-Holland, Amsterdam, 1991), pp. 210–223.
- ⁹P. W. Stephens *et al.*, *Nature* **351**, 632 (1991).
- ¹⁰S. C. Erwin and W. E. Pickett, *Science* **254**, 842 (1991).
- ¹¹P. B. Allen, T. P. Beaulac, F. S. Khan, W. H. Butler, F. J. Pinski, and J. C. Swihart, *Phys. Rev. B* **34**, 4331 (1986).
- ¹²R. A. Jishi and M. S. Dresselhaus, *Phys. Rev. B* **45**, 2597 (1992).
- ¹³M. Schluter, M. Lannoo, M. Needles, and G. A. Baraff, *Phys. Rev. Lett.* **68**, 526 (1992).
- ¹⁴C. M. Varma, J. Zaanen, and K. Raghavachari, *Science* **254**, 989 (1991).
- ¹⁵W. L. McMillan, *Phys. Rev.* **167**, 331 (1968).
- ¹⁶W. E. Pickett, *Bull. Am. Phys. Soc.* **37**, 455 (1992).
- ¹⁷O. V. Dolgov and I. I. Mazin, *Solid State Commun.* **81**, 935 (1992).
- ¹⁸F. C. Zhang, M. Ogata, and T. M. Rice, *Phys. Rev. Lett.* **67**, 3452 (1991).
- ¹⁹K. Prassides, J. Tomkinson, C. Christides, M. J. Rosseinsky, D. W. Murphy, and R. C. Haddon, *Nature* **354**, 462 (1991).
- ²⁰J. P. Carbotte, *Rev. Mod. Phys.* **62**, 1067 (1990).
- ²¹Z. Zhang, C.-C. Chena, and C. Lieber, *Science* **253**, 1 (1991).
- ²²L. D. Rotter, Z. Schlesinger, J. P. McCauley, Jr., N. Coustel, J. E. Fischer, and A. B. Smith, III, *Nature* **355**, 532 (1992).
- ²³L. Degiorgi, P. Wachter, G. Grüner, S.M. Huang, J. Wiley, and R.B. Koner (unpublished).